© 2019. Published by The Company of Biologists Ltd | Journal of Cell Science (2019) 132, jcs233429. doi:10.1242/jcs.233429

RESEARCH ARTICLE

The *Chlamydomonas* flagellar membrane glycoprotein FMG-1B is necessary for expression of force at the flagellar surface

Robert A. Bloodgood[1], Joseph Tetreault[2,*] and Roger D. Sloboda[2,3,‡]

ABSTRACT

In addition to bend propagation for swimming, *Chlamydomonas* cells use their flagella to glide along a surface. When polystyrene microspheres are added to cells, they attach to and move along the flagellar surface, thus serving as a proxy for gliding that can be used to assay for the flagellar components required for gliding motility. Gliding and microsphere movement are dependent on intraflagellar transport (IFT). Circumstantial evidence suggests that mechanical coupling of the IFT force-transducing machinery to a substrate is mediated by the flagellar transmembrane glycoprotein FMG-1B. Here, we show that cells carrying an insertion in the 5′-UTR of the FMG-1B gene lack FMG-1B protein, yet assemble normal-length flagella despite the loss of the major protein component of the flagellar membrane. Transmission electron microscopy shows a complete loss of the glycocalyx normally observed on the flagellar surface, suggesting it is composed of the ectodomains of FMG-1B molecules. Microsphere movements and gliding motility are also greatly reduced in the 5′-UTR mutant. Together, these data provide the first rigorous demonstration that FMG-1B is necessary for the normal expression of force at the flagellar surface in *Chlamydomonas*.

This article has an associated First Person interview with authors from the paper.

KEY WORDS: *Chlamydomonas*, FMG-1B, Flagella, Cilia, Flagellar membrane, Gliding motility, Surface motility

INTRODUCTION

FMG-1B is the major membrane glycoprotein in the flagella of the bi-flagellate green alga, *Chlamydomonas*, as determined by SDS-PAGE (Witman et al., 1972). Biotinylation studies show that FMG-1B is exposed at the flagellar surface (Bloodgood, 1990), and immobilized iodination studies have demonstrated that FMG-1B is the only flagellar protein in contact with the substrate during whole-cell gliding motility and microsphere movement (Bloodgood and Workman, 1984). The nascent protein is composed of 4389 residues, including an N-terminal signal sequence, and exhibits N-linked glycosylation at multiple sites. FMG-1B has a single transmembrane domain at amino acid residues 4340–4372, resulting in a very short cytoplasmic domain of 17 residues. The heavily glycosylated ectodomain of FMG-1B is presumed to comprise the prominent glycocalyx observed on flagella by electron microscopy (Bloodgood and May, 1982). Despite its large size and evidence for its involvement in transmembrane signaling (Bloodgood and Salomonsky, 1994), FMG-1B possesses a relatively short (17 residues) cytoplasmic domain extending into the flagellar matrix. Preliminary reports have identified a number of putative binding partners for the FMG-1B cytoplasmic tail, including cytoplasmic dynein 1B, a gliding-associated kinase (GAK), FAP12 and FAP113 (Betleja, 2012; Bloodgood, 2009; Bloodgood and Salomonsky, 1994; Kamiya et al., 2018).

Chlamydomonas exhibits four types of flagella-dependent motility. First, cells can swim forward (flagella leading the cell body), in which case the flagella produce a power stroke followed by a recovery stroke, similar to cilia in the human airway. Second, cells can reverse direction by switching to a symmetrical sine wave form of flagellar motility similar to that of sperm tail flagella (flagella trailing the cell body); switching between the two beat patterns is controlled by changes in the intraflagellar Ca^{2+} concentration (Bessen et al., 1980; Schmidt and Eckert, 1976). Third, in moist soil, on an agar plate or on a microscope slide, the flagellar surface can interact with the substrate facilitating whole-cell gliding motility (with the active flagellum leading and the passive flagellum trailing). A fourth flagellum-dependent motility mechanism, called intraflagellar transport or IFT (Kozminski et al., 1993), moves multisubunit protein complexes called IFT trains from the flagellar base to the tip (anterograde direction) and back from the flagellar tip to the base (retrograde direction). Anterograde IFT is powered by the activity of kinesin 2, which uses the lattice of the B tubule of the outer doublets as the substrate; retrograde IFT is powered by cytoplasmic dynein 1b/2 and uses the lattice of the A tubule of the outer doublet as the substrate (Rosenbaum and Witman, 2002; Stepanek and Pigino, 2016). IFT trains carry cargo, such as tubulin dimers, radial spokes and axonemal dynein arms, to the flagellar tip for assembly and maintenance of the organelle. Although it is normally distributed evenly along the surface of the flagellum, FMG-1B also serves as a cargo for the IFT machinery (Shih et al., 2013), albeit an unusual cargo because the association of FMG-1B with the IFT trains is regulated by a transmembrane signaling pathway (initiated by FMG-1B cross-linking) involving Ca^{2+} influx (Bloodgood and Salomonsky, 1990) and changes in the state of protein phosphorylation (Bloodgood and Salomonsky, 1994).

In addition to its classic role in flagellar assembly and maintenance, IFT has recently been shown to function in gliding motility and movement of polystyrene microspheres, which can attach to and move along the flagellar surface, and thus serve as a proxy for gliding (Shih et al., 2013). Microspheres moved only when colocalized with a moving IFT train; reversal of direction of microsphere movement occurred when a microsphere switched from an anterograde to a retrograde train or vice versa (Shih et al., 2013). Bloodgood and Salomonsky (1998) have previously shown

[1]Department of Cell Biology, University of Virginia School of Medicine, Charlottesville, VA 22908, USA. [2]Department of Biological Sciences, Dartmouth College, Hanover, NH 03755, USA. [3]The Marine Biological Laboratory, Woods Hole, MA 02543, USA.
*Present address: Department of Agriculture, Nutrition, and Food Science, University of New Hampshire, Durham, NH 03824, USA.

‡Author for correspondence (rds@dartmouth.edu)

R.D.S., 0000-0001-6077-8947

Received 18 April 2019; Accepted 23 July 2019

Journal of Cell Science (2019) 132, jcs233429. doi:10.1242/jcs.233429

that microsphere attachment induced FMG-1B clustering in the flagellar membrane. In order to implicate IFT movement as the underlying force for whole-cell gliding motility, Shih et al. (2013) showed that retrograde IFT trains would occasionally stall (due to adhesion to the substrate) and, only during the period of time that the train remained stationary relative to the substrate, would the cell exhibit gliding motility relative to the substrate. Using a temperature-sensitive (ts) strain in cytoplasmic dynein 1b/2 and a small-molecule inhibitor of this dynein, these same authors have clearly shown that gliding motility is dependent on cytoplasmic dynein 1b/2 activity, the same motor responsible for retrograde IFT. How might the movement of IFT trains, located between the outer surface of the outer doublets and the inner surface of the flagellar membrane, apply force to an extracellular substrate? The presumption from previous studies (e.g. Bloodgood and Workman, 1984) was that the transmembrane flagellar glycoprotein FMG-1B mechanically coupled flagellar retrograde IFT trains to the extracellular substrate along which the cell glides (or to the surface of a microsphere).

Despite a great deal of circumstantial evidence, it has never been directly demonstrated that FMG-1B is the flagellar component that mediates IFT motor-dependent force transduction at the flagellar surface. In this report, we demonstrate that a specific insertional mutant cell line from the *Chlamydomonas* CLiP library (Li et al., 2016) (1) fails to express the FMG-1B protein in flagella, as demonstrated by immunoblots of isolated flagella; (2) does not stain with antibodies to FMG-1B under conditions in which wild-type (wt) cells are strongly stained; (3) no longer has the glycocalyx characteristic of the flagellar surface of wt cells; (4) can still assemble and regenerate full-length flagella despite the absence of FMG-1B, albeit with kinetics that are somewhat slower than that exhibited by wt cells; (5) is defective in flagellar surface motility as measured by a microsphere movement assay; and (6) is unable to glide along a substrate or even assume the normal gliding morphology, in which the flagella are oriented 180° to each other. From these data, we conclude that FMG-1B is essential for the transduction of force at the flagellar surface resulting in microsphere movement and whole-cell gliding motility.

RESULTS

We obtained two insertional mutants from a CLiP Library (Li et al., 2016), which we refer to here as strain 47 and strain 56. As demonstrated by PCR analysis (Fig. 1A), strain 47 carries an insertion in the 3′-UTR, while strain 56 carries an insertion in the 5′-UTR of the gene encoding FMG-1B, thus confirming the information

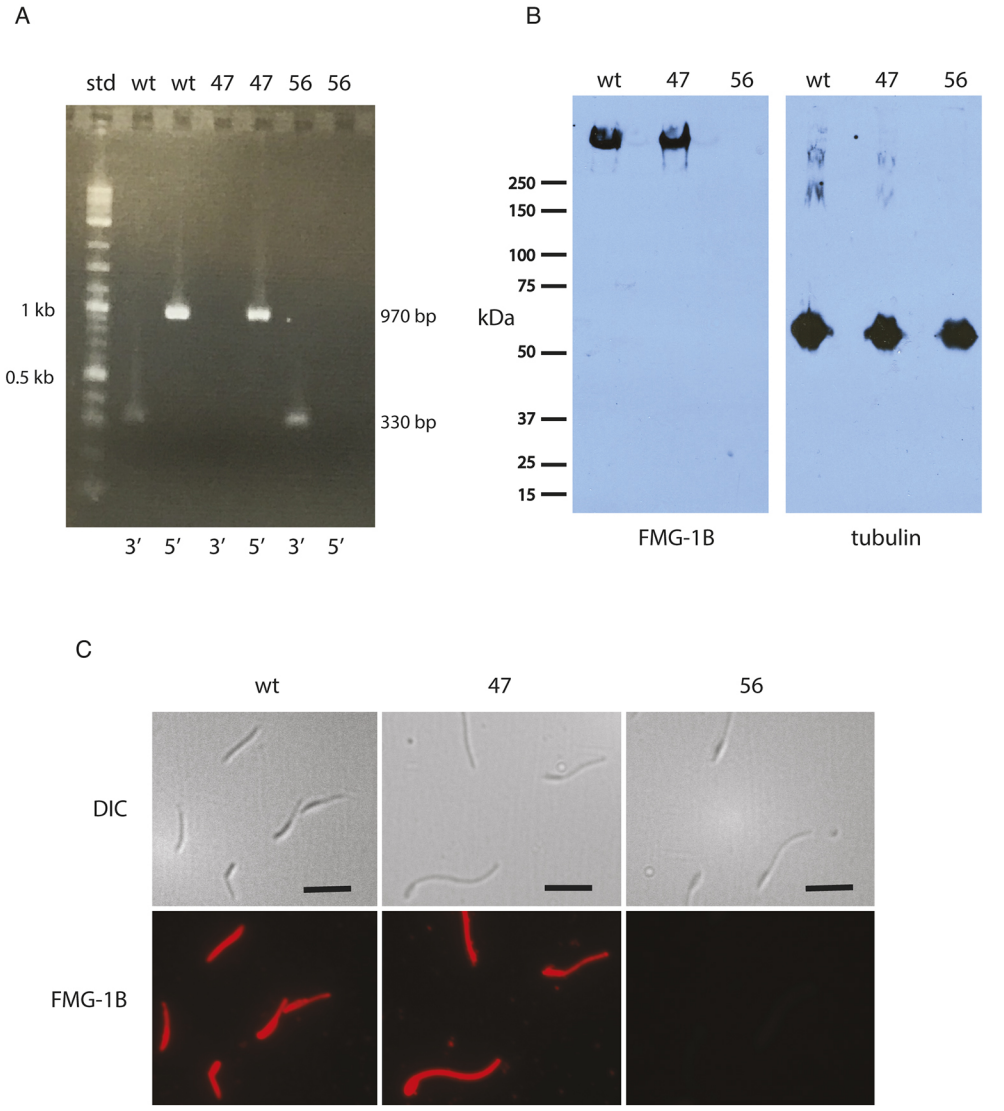

Fig. 1. Analysis of key features of the cell strains used in this study. (A) Strain 47 contains an insertion in the 3′-UTR between nts 14,379 and 14,380 relative to the start ATG; strain 56 contains an insertion in the 5′-UTR, between nts –157 and –158 relative to the start ATG. This figure shows PCR data using 3′- and 5′-UTR-specific primers. The 3′-UTR primers (sequences listed in the Materials and Methods), which flank the insertion site, produce a product of 330 bp in wt and strain 56 cells, but not in strain 47 cells. Conversely, 5-UTR-specific primers produce an expected product of 970 bp in wt and strain 47 cells, but not in strain 56 cells. The figures on the left indicate positions of two relevant markers in the standards lane, while the figures on the right indicate the expected sizes of the PCR products. (B) These immunoblots analyze samples of flagella purified from the cell strains indicated. The left panel has been reacted with a monoclonal antibody (#61) that is specific for FMG-1B on immunoblots. Under these conditions, FMG-1B is undetectable in strain 56 while it is present at a wt level in flagella from strain 47. The blot was then stripped and reprobed with antibodies to α-tubulin to serve as a loading control (right panel). (C) Isolated flagella were fixed and stained with an anti-carbohydrate monoclonal antibody (#8) that is specific for FMG-1B via immunofluorescence. The monoclonal antibody (#61) used for immunoblots does not react with FMG-1B in intact flagella because its peptide epitope is occluded by the extensive glycosylation of FMG-1B. Scale bars: 5 µm.

Journal of Cell Science (2019) 132, jcs233429. doi:10.1242/jcs.233429

provided (https://www.chlamylibrary.org/). The results, using wt DNA as the template, show the predicted sizes of 330 bp for the 3′-UTR-specific primers and 970 bp for the 5′-UTR-specific primers (Fig. 1A). The 330 bp fragment cannot be amplified from template DNA isolated from strain 47, and the 970 bp fragment cannot be amplified using strain 56 DNA as template. The lack of a PCR-specific product for each mutant strain indicates the insertion is too large (the mutagenesis cassette is ∼2660 bp) or too complex (Li et al., 2016) to be amplified under the conditions used, or that a deletion has occurred in this region of the gene. Our data do not allow a determination of which possibility is occurring in strain 47 and 56.

We next analyzed, though immunoblotting, wt and mutant flagella for the presence of FMG-1B protein (Fig. 1B). As predicted by the PCR results, and suggested by the reported locations of the insertions, both wt and strain 47 flagella contain similar levels of FMG-1B. However, FMG-1B protein is undetectable by immunoblotting in flagella from strain 56 cells. The lack of FMG-1B protein in strain 56 flagella is also supported by immunofluorescence analysis. When flagella are isolated and stained with a monoclonal antibody to FMG-1B, both wt and strain 47 flagella stain intensely; flagella isolated from strain 56 cells show no detectable staining with FMG-1B antibodies (Fig. 1C). One reason strain 56 cells lack detectable FMG-1B might be because the insertion in the 5′-UTR disrupts the ribosome-binding site in the FMG-1B mRNA (Gebauer et al., 2012) and hence translation of the FMG-1B message does not occur. Alternatively, the mRNA produced may be unstable and thus degrade quickly. Our data do not distinguish between these two possibilities, but we note that, on occasion, we have detected by immunoblotting (see Fig. S1) a small amount of full-length FMG-1B in flagella isolated from strain 56 cells. Thus, the inability of strain 56 cells to synthesize FMG-1B is not absolute. The data reported in the figures in this paper have been obtained with cells lacking detectable FMG-1B as judged by immunoblotting.

Chlamydomonas flagella have a prominent glycocalyx assumed to be composed of the highly glycosylated ectodomain of FMG-1B. The glycocalyx can be seen very clearly in thin-section electron microscope images of wt and strain 47 cells that express FMG-1B (Fig. 2, top and middle panels). However, the glycocalyx is completely absent in the flagella of strain 56 cells (bottom). These combined data from PCR, immunoblotting, immunofluorescence and electron microscopy indicate that strain 56 cells contain little, if any, FMG-1B in the flagellar membrane. We next sought to determine how the loss of FMG-1B affected flagellar assembly and surface-dependent flagellar functions.

Surprisingly, strain 56 cells, although they lack the major protein component of the flagellar membrane, still assemble near full-length flagella with kinetics that are similar to wt cells. The rate at which the flagella assemble is decreased slightly in the absence of FMG-1B, as shown in Fig. 3. Here, cells have been deflagellated and allowed to regenerate their flagella. At various time points, aliquots were fixed, and the average length of 50 flagella at each time point was determined. The rate of assembly of flagella in strain 56 cells (∼0.09 µm/min) lags slightly behind that of wt cells (∼0.12 µm/min); in addition, strain 56 cells reach their maximum length at 240 min post deflagellation, as compared to 120 min for wt cells. At 5 h following deflagellation, wt cells have regenerated flagella that are 81% of their pre-deflagellation length, while strain 56 cells have reached 76%. Thus, the regenerative ability and final flagellar length are similar for both cell types, regardless of the presence or absence of FMG-1B.

There are two assays available that are generally accepted as proxies for flagellar gliding motility. These involve a measure of the ability of flagella to bind and translocate polystyrene microspheres along the flagellar surface, and the ability of cells to adopt the gliding configuration. For the former assay (see Movie 1), the movement of polystyrene microspheres along the flagella has been demonstrated to depend on the same motor activity responsible for gliding motility, as shown by Shih et al. (2013). The microsphere assay was conducted on wt and both mutant strains (Fig. 4A,B). In wt and strain 47 cells, the majority of flagella assayed had microspheres that were bound and/or moving (Fig. 4A); on average, wt cells had 0.79 microspheres bound per flagellum, and strain 47 cells had 0.96 microspheres bound per flagellum. By contrast, strain 56 cells had an average of only 0.18 microspheres bound per flagellum (Fig. 4B). In addition, 63.2% of the flagella in strain 56 cells had no microspheres bound, compared to 19.5% and 13.7% for wt and strain 47 cells, respectively. Note that in a given sample, the number of flagella with microspheres bound is a function of the ratio of microspheres to flagella in the assay. The greater the concentration of microspheres in the assay, the more that will bind to the flagella surface. The data summarized above were obtained with the same concentration of microspheres and cells for each strain assayed (see Materials and Methods for details). We conclude, therefore, that the loss of FMG-1B in strain 56 cells results in a dramatic reduction in microsphere binding and motility.

A similar difference between wt and mutant cells is evident when cells are scored as to whether or not they adopt a gliding morphology on the microscope slide (Fig. 4C,D). For images of cells that have adopted the gliding morphology, see Fig. S2. As quantified in Fig. 4C, wt and strain 47 cells, which express similar levels of FMG-1B (Fig. 1B), adopted the gliding morphology to a similar extent (Fig. 4C). Within minutes of being placed on the slide, 65.2% of wt cells and 71.6% of strain 47 cells have their flagella positioned 180° opposed to each other. By contrast, only 26.4% of strain 56 cells assume the gliding configuration within the same time period (Fig. 4D). Collectively, the data presented in Fig. 4 clearly demonstrate a requirement for FMG-1B in flagellar surface motility.

DISCUSSION

While many forms of cell motility involve the transduction of force at the cell surface, often involving the actin cytoskeleton and integrin proteins in the plasma membrane in the case of metazoan cells, there is a special class of motility that occurs at the surface of some membrane protrusions. Specifically, surface motility is exhibited on cytoplasmic protrusions that contain arrays of microtubules in certain eukaryotic protists and metazoans. Surface motility associated with these structures can be visualized by the addition of inert particles, such as polystyrene microspheres, whose microtubule-dependent movements on the cell surface have been demonstrated in numerous organisms: the haptonema of Prymnesiophycean flagellate protozoa (Kawachi et al., 1991), the axopodia of Heliozoan protozoa (Bardele, 1976; Bloodgood, 1977; Kanno and Ishii, 1979; Troyer, 1975), the reticulopodia of Foraminiferan protozoa (Bowser and Bloodgood, 1984; Bowser et al., 1984), the flagella of algae (Bloodgood, 1977; Lewin, 1982), the leading flagellum of *Peranema* (Saito et al., 2003), the balancer cilia of ctenophores (Noda and Tamm, 2014) and the cilia of sea urchin blastulae (Bloodgood, 1980; Kamiya et al., 2018). The postulated physiological roles for force transduction at the surfaces of these microtubule-containing extensions of the plasma membrane include: prey organism capture and transport to the cell body for phagocytosis (Kawachi et al., 1991; Suzaki et al., 1980), movement of whole cells (lithocytes) along cilia in ctenophores (Noda and Tamm, 2014), mating of flagellated gametes in

Journal of Cell Science (2019) 132, jcs233429. doi:10.1242/jcs.233429

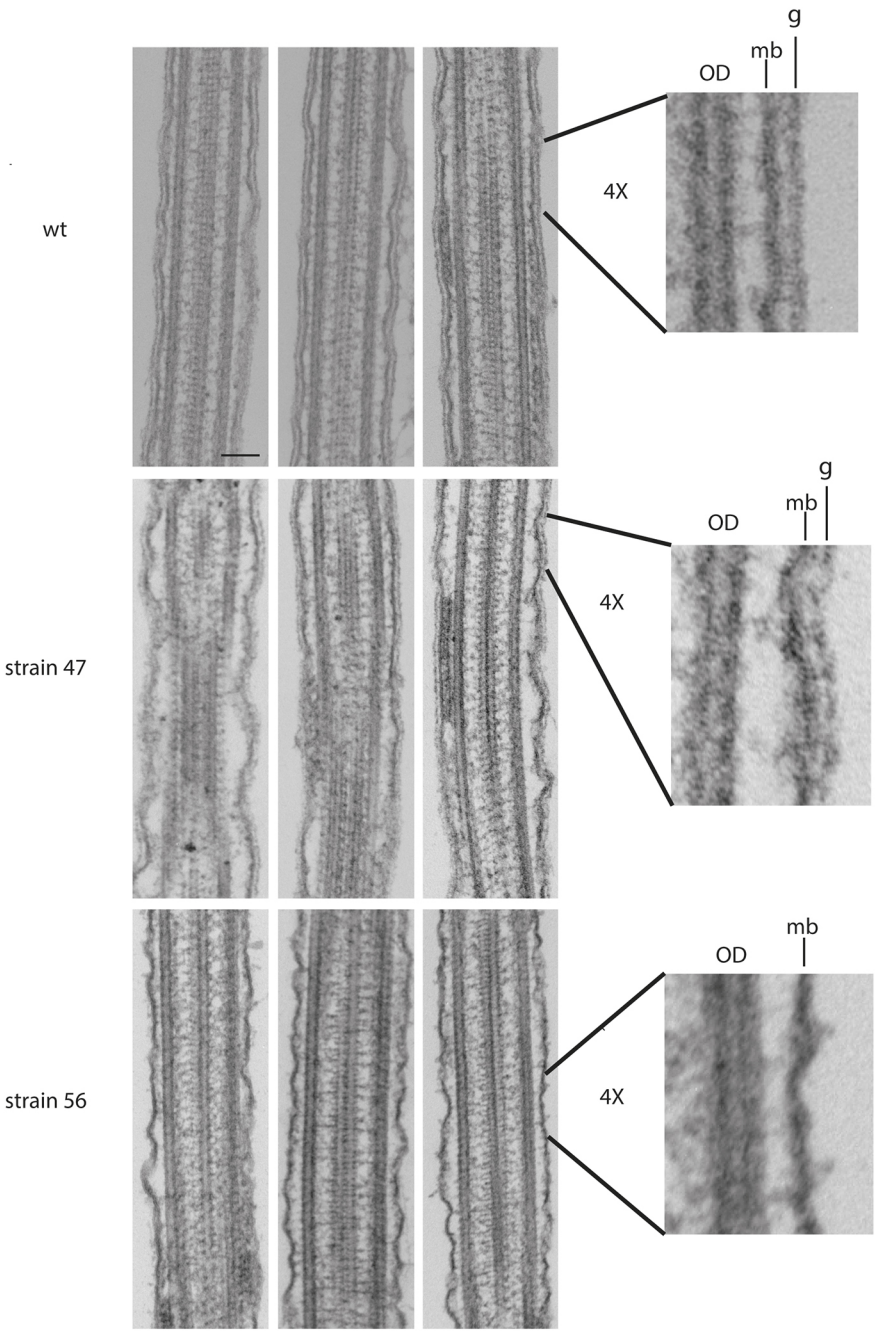

Fig. 2. Thin-section electron microscopy. Longitudinal sections of three flagella isolated from each of the three cell strains: wt, strain 47 and strain 56. The panels on the right show selected regions as indicated that have been enlarged by a factor of 4×. OD, outer doublet microtubule; mb, flagellar membrane; g, glycocalyx. Scale bar: 100 nm (applies to all panels on the left).

Chlamydomonas (Hoffman and Goodenough, 1980; Snell et al., 1982), removal of debris from the surface of motile cilia, which may interfere with the hydrodynamics of ciliary beating, and flagella-dependent whole-cell gliding motility (Bloodgood, 1981; Lewin, 1952; Mast, 1912; Saito et al., 2003; Shih et al., 2013; Ulehla, 1911).

Flagellar surface motility and its association with whole-cell gliding motility has been studied most extensively in *Chlamydomonas* (Bloodgood, 2009; Bloodgood and Salomonsky, 1990), although it has also been clearly demonstrated in *Peranema* (Saito et al., 2003). All gliding defective mutants of *C. moewusii* (Lewin, 1982; Reinhart and Bloodgood, 1988) and many gliding-defective mutants of *C. reinhardtii* (Kozminski, 1995) are also defective in microsphere adhesion and/or movement, suggesting that the same force transduction mechanism operating at the flagellar surface is responsible for both microsphere movements and gliding motility. Microsphere movement and gliding motility in *Chlamydomonas* are both dependent on micromolar concentrations of Ca^{2+} in the medium (Bloodgood et al., 1979; Kozminski et al., 1993).

The principal flagellar membrane protein in *Chlamydomonas* is a large glycoprotein called FMG-1B. It is a highly N-glycosylated, 410 kDa integral membrane protein whose gene is located at the left end of chromosome 9. The GenBank accession number is AY208914.2 and the gene construct in Phytozome 13 is Cre09.g392867.t1.1. Immobilized iodination experiments have shown that FMG-1B is the only detectable protein that contacts the microsphere surface during microsphere movement and the only flagellar protein that contacts the slide or coverslip surface during gliding motility (Bloodgood and Workman, 1984). Clustering of FMG-1B within the plane of the flagellar membrane by FMG-1B antibodies or the

Journal of Cell Science (2019) 132, jcs233429. doi:10.1242/jcs.233429

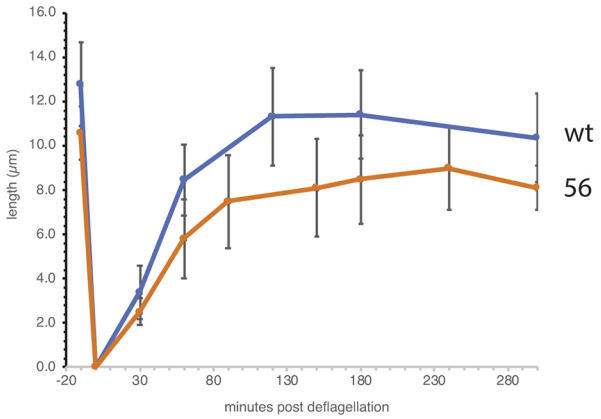

Fig. 3. The lack of FMG-1B does not inhibit flagellar growth or regeneration. The mean length of flagella for wt and strain 56 cells is shown at the −10 min time point. The cells were then deflagellated (*t*=0) and allowed to regenerate as described in the Materials and Methods section. At specific time points after deflagellation, cells were fixed and flagellar lengths were measured using the length measurement tool in Metamorph. For each time point noted, 50 flagella were measured, and the mean±s.d. length was plotted. The mean flagella length prior to deflagellation was: wt cells, 12.8±1.9 µm; strain 56 cells, 10.6±1.2 µm. The mean flagellar length 5 h after deflagellation was: wt cells, 10.4±2.0 µm; strain 56 cells, 8.1±1.0 µm.

lectin Concanavalin A induces the directed movement of these protein clusters along the flagellar surface (Bloodgood et al., 1986). The cross-linking-induced movement of FMG-1B within the flagellar membrane is reversibly inhibited by removing Ca^{2+} from the medium, or by the addition of Ca^{2+} channel blockers, calmodulin antagonists, protein kinase inhibitors and protein phosphatase inhibitors (Bloodgood, 1990, 1992; Bloodgood and Salomonsky, 1990, 1991, 1994). When the FMG-1B glycoproteins were extensively crosslinked so as to prevent their translocation within the flagellar membrane, microsphere movements and gliding motility were inhibited (Bloodgood and Salomonsky, 1989). *In vivo* phosphorylation studies have shown that crosslinking of FMG-1B using specific monoclonal antibodies, Concanavalin A or polystyrene microspheres induces specific changes in the phosphorylation state of a small number of flagellar phosphoproteins. The most dramatic change is the complete dephosphorylation of a 55 kDa phosphoprotein that co-immunoprecipitates with FMG-1B (Bloodgood and Salomonsky, 1994, 1998).

These data led to a hypothesis for gliding motility (Bloodgood, 2009) in which cross-linking and clustering of FMG-1B induces a signaling pathway involving an influx of Ca^{2+}, activating a Ca^{2+}- and calmodulin-dependent protein kinase and/or phosphatase, resulting in a change in the phosphorylation state of a few flagellar proteins. These changes in turn induce mechanical coupling of FMG-1B clusters to force-transducing machinery inside the flagellum. Attempts to move the FMG-1B cluster through the flagellar membrane and along the length of the flagellum while it is adherent to the substrate results in translocation of the cell (or of a microsphere along the surface of the flagellum) (Bloodgood, 2009; Shih et al., 2013).

What machinery is responsible for force transduction at the flagellar surface? For surface motility, FMG-1B performs a role analogous to that played by integrins in metazoan motility. For example, migrating cells adhere to the extracellular matrix (ECM), and trans-membrane proteins, the integrins, mediate the interaction of cytoplasmic actin filaments with laminin in the ECM (Huttenlocher and Horwitz, 2011). Cross-linking of integrins within the plasma membrane results in protein phosphorylation. Kozminski and colleagues (Kozminski et al., 1993) reported on a new type of motility associated with the *Chlamydomonas* flagellum and named it intraflagellar transport (IFT). IFT has been demonstrated to occur in virtually all eukaryotic cilia and flagella and is necessary for flagellar protein turnover and the maintenance of normal flagellar length. Mutations in and inhibitors of IFT motor proteins result in loss of microsphere movement and gliding motility (Kozminski et al., 1995; Laib et al., 2009; Shih et al., 2013).

Twenty years after the discovery of IFT, the Yildiz laboratory (Shih et al., 2013) clearly demonstrated that IFT was responsible for both microsphere movements and flagella-dependent whole-cell gliding motility in *Chlamydomonas*. In doing so, they resolved the three discrepancies between the characteristics of IFT and flagellar surface motility mentioned previously. IFT trains bound to a polystyrene microsphere move at the velocity characteristic of microsphere movements and not that of typical IFT trains. The saltatory movement of microspheres can be explained by microspheres releasing from an IFT train and then reattaching to another IFT train, which could be moving in the same or the opposite direction. While the mechanism of IFT does not require Ca^{2+}, the mechanical coupling (via FMG-1B) of the IFT machinery to microspheres during microsphere movement or substrate contact sites during whole-cell gliding does require a Ca^{2+}-activated signaling pathway, unlike coupling of IFT to other known IFT cargo.

Shih et al. (2013) used microspheres coated with antibodies to FMG-1B to show that the microspheres colocalize with IFT trains during both anterograde and retrograde processive runs along the *Chlamydomonas* flagellum. For an excellent illustration of the interaction between an outer doublet, an IFT train, FMG-1B, and an extracellular surface (in this case a microsphere), refer to Fig. 1D in Shih et al. (2013). Although these authors assumed that their FMG-1B antibody-coated microspheres recruited FMG-1B which functioned to couple the microsphere to IFT trains, they did not directly demonstrate this and provided no direct evidence that FMG-1B was essential for microsphere movement or gliding motility in *Chlamydomonas*.

With a few exceptions (Rosenbaum and Witman, 2002), IFT is required for the assembly and maintenance of all cilia and flagella. What is currently unclear is whether IFT is present in and responsible for all types of surface motility associated with microtubule-filled extensions (haptonema, axopodia, reticulopodia, cilia and flagella). Because IFT appears to be active in all eukaryotic cilia and flagella, it is strongly suspected (albeit not proved) that IFT is the driving force for all documented cases of microsphere movements and gliding motility associated with cilia and flagella. What is much less clear is whether IFT is associated with surface movements of microspheres and prey organisms in the non-cilia/flagella cases involving haptonema, axopodia and reticulopodia. In studying the genome of the foraminiferan *Reticulomyxa* [which clearly shows microsphere and prey organism movements along the surface of the reticulopodial network, Glöckner et al. (2014) identified genes for the anterograde and retrograde IFT motors (kinesin-2 and cytoplasmic dynein 1b, respectively)] as well as quite a few IFT proteins (IFT88, IFT57, IFT140, IFT172, IFT80 and IFT20); however, based on RNAseq and EST data, these IFT proteins do not appear to be expressed. Although the gene for FMG-1B is found only in *Chlamydomonas* and closely related members of the volvocine line of green algae, it is certainly possible that other plasma membrane proteins serve to mechanically couple IFT trains and the cell surface in other microtubule-filled cell extensions that display surface motility.

Journal of Cell Science (2019) 132, jcs233429. doi:10.1242/jcs.233429

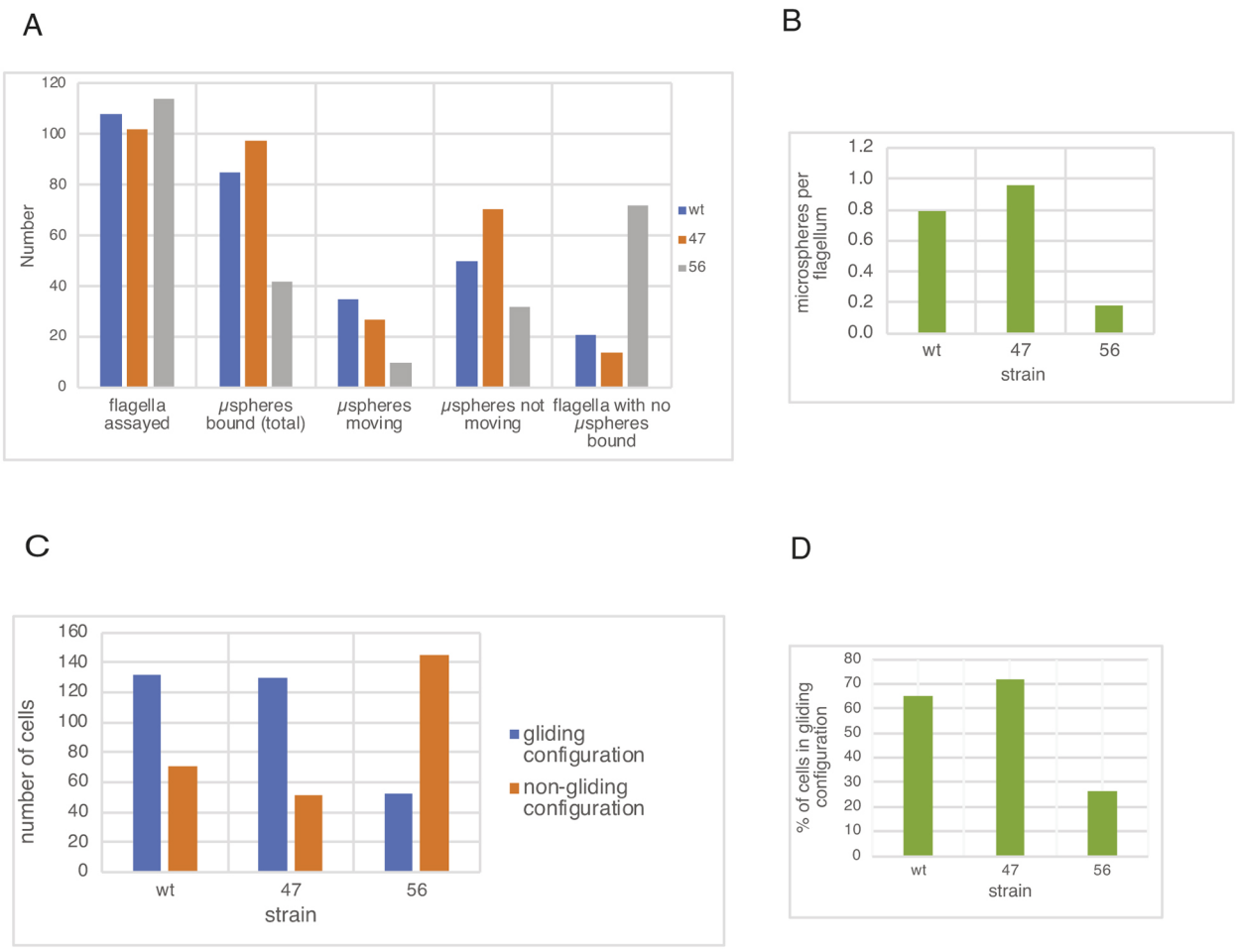

Fig. 4. Cells lacking FMG-1B are deficient in their ability to exhibit microsphere binding and/or movement, and are unable to adopt the gliding conformation. (A) Assessment of microsphere binding and movement. wt, strain 47 and strain 56 flagella were assayed for the ability to bind and translocate polystyrene microspheres (μspheres) along the flagellar surface. The data shown are an average of two experiments. The number of microspheres bound and moving can exceed the number of flagella assayed because more than one microsphere can bind to a single flagellum. *n*=215 (wt), 204 (strain 47), and 226 (strain 56). (B) Number of microspheres bound per flagellum. The average number of microspheres bound per flagellum is shown for wt, strain 47 and strain 56 cells. (C) Cells lacking FMG-1B are deficient in their ability to adopt the morphology characteristic of gliding cells. wt (*n*=188), strain 47 (*n*=195) and strain 56 (*n*=179) cells were assayed for the ability to adopt a gliding configuration in which the cells adhere to the slide with their flagella oriented 180° relative to each other. The data shown here are the mean values from two experiments. D. The same data as in C, plotted to show the percentage of cells in a given population that adopt the gliding configuration.

Despite all the circumstantial evidence implicating FMG-1B in the mechanism responsible for gliding motility and microsphere movement in *Chlamydomonas reinhardtii*, no definitive demonstration of this has yet been published. In the present study, we have utilized a strain of *Chlamydomonas reinhardtii* with an insertional mutation in the 5′-UTR (designated strain 56) (Li et al., 2016) to dissect the role of FMG-1B in microsphere movement and gliding motility. By several independent criteria, we have demonstrated that strain 56 lacks FMG-1B (Fig. 1) as well as the prominent glycocalyx evident in wt cells (Fig. 2). Because the 5′-UTR is required for proper interaction of mRNA with the ribosome, this might explain the lack of detectable FMG-1B in flagella isolated from strain 56 cells. These data demonstrate for the first time that the flagellar glycocalyx is composed primarily of the large and highly glycosylated ectodomains of FMG-1B proteins (only 17 of the 4149 residues of FMG-1B are cytoplasmic). Cells lacking the major protein component of the flagellar membrane are still able to grow flagella, and to regenerate them with kinetics very similar to wt cells (Fig. 3).

Strain 56 also exhibits a reduction in microsphere adhesion to the flagellar surface and an even more dramatic reduction in the motility of microspheres associated with the flagellar surface, while strain 47 resembles the wt parent strain in terms of microsphere attachment and motility (Fig. 4A,B). Flagella-dependent gliding motility in *Chlamydomonas* always involves the flagella contacting a planar substrate and then the cell assuming a very characteristic gliding configuration with the two flagella oriented 180 degrees to one another. Non-gliding mutants and wt cells treated with inhibitors of surface motility are unable to assume this characteristic gliding configuration. Because of the ease with which this morphology can be quantified, we used gliding conformation as an assay to compare wt and mutant strains. Strain 56, which lacks FMG-1B, exhibited a dramatic reduction in its ability to assume the gliding configuration (Fig. 4C,D). Together, our observations demonstrate that the FMG-1B flagellar membrane glycoprotein is necessary for flagellar surface motility (microsphere movement and gliding motility) in *Chlamydomonas reinhardtii*.

Journal of Cell Science (2019) 132, jcs233429. doi:10.1242/jcs.233429

One final point needs to be addressed here. If FMG-1B is entirely absent, why is there any microsphere binding and movement on, or assumption of the gliding configuration, by strain 56 flagella? There are several possible explanations. Perhaps only a very small number of FMG-1B molecules are actually required to bind a microsphere or a coverslip. If true, and if some cells of strain 56 synthesized a very small (undetectable by immunoblotting) amount of FMG-1B, this may be sufficient to support a low level of substrate binding as detected by the assays used to generate the data shown in Fig. 4. Alternatively, microsphere binding and gliding may not be solely dependent on FMG-1B, and in its absence other minor flagellar membrane proteins may become accessible for substrate binding and fulfill the same role as FMG-1B. In the three cell strains used here, the IFT-based motor machinery required for surface and gliding motility is completely functional. If a membrane protein (other than FMG-1B), which might normally be prevented from substrate contact by the presence of the glycocalyx, could both adhere to a microsphere surface or a planar glass substrate and also serve as cargo for the IFT machinery, one might expect to see some microsphere movement and/or gliding in the absence of FMG-1B. When raising monoclonal antibodies to FMG-1B, we also obtained antibodies that recognized membrane glycoproteins that were minor components of the flagellar membrane. One of these antibodies was able to induce clustering and movement (capping) of its target protein, indicating the ability of at least one other membrane protein, in addition to FMG-1B, to interact with force transduction machinery within the flagellum (data not shown). Similarly, more-recent studies have demonstrated the role of IFT-A complexes in the movement of peripheral as well as integral membrane proteins into the flagellum; the latter include the polycystin 1 and 2 complex, TRPV channels, and various classes of G-protein-coupled receptors (Qin et al., 2005; Huang et al., 2007; Shih et al., 2013; Hirano et al., 2017; Morthorst et al., 2018). There is also evidence that at least some ciliary membrane proteins are not dependent upon IFT for entry into and movement within the ciliary membrane (Ye et al., 2013; Belzile et al., 2013). With respect to gliding motility, the possibility exists that other membrane proteins, because they interact with IFT-A, which is responsible for retrograde IFT (Picariello et al., 2019), may also be able to function in gliding. This might occur if these proteins become more readily able to interact with the surface of a substrate once FMG-1B (which possesses a very large glycosylated ectodomain) is no longer present. Such a situation might explain the limited amount of microsphere movement and gliding morphology observed in strain 56 cells (Fig. 4).

MATERIALS AND METHODS

Cells and culture conditions

Chlamydomonas reinhardtii CC5325 (wild type, wt) and the insertional mutant strains LMJ.SG0182.001447 and LMJ.SG0182.002356 (herein referred to as strains 47 and 56, respectively) were obtained from the *Chlamydomonas* library project (CLiP; Li et al., 2016). Cultures were maintained on 1% agarose in tris-acetate-phosphate (TAP) medium; on some occasions the agarose for 47 and 56 cells also contained 20 µg/ml paromomycin, the selection agent for the insertion cassette. For an experiment, cells were transferred to 500 ml or 1 liter flasks of M medium (Sager and Granick, 1953); again, on some occasions 20 µg/ml paromomycin was added to the cultures of 47 and 56 cells. All growth conditions were at 23°C under a cycle of 14 h of light and 10 h of dark, with aeration.

Isolation of flagella

Cells in M medium were centrifuged for 5 min at 1056 ***g*** using a Sorvall GS-3 rotor. The supernatant was discarded, and the pellet resuspended in TAP medium. Full-length flagella were detached from the cell body by pH shock. Cells were stirred as the pH was rapidly decreased to 4.5 using 0.5 M acetic acid; after 1 min at pH 4.5, the pH was rapidly returned to the starting level of 7.3 by the addition of 0.5 M KOH (Witman et al., 1972). Cell bodies were sedimented in a GS-3 rotor for 5 min at 1056 ***g***. The supernatant containing the flagella was then centrifuged for 10 min at 9224 ***g*** in a Sorvall HB-4 rotor and resuspended in several milliliters of HMDEK (10 mM HEPES [4-(2-hydroxyethel)-1-piperazineethanesulfonic acid], pH 7.5, 5 mM $MgSO_4$, 1 mM dithiothreitol, 0.5 mM ethylene glycol tetraacetic acid, 25 mM potassium acetate). The resuspended flagella were underlaid with HMDEK containing 6% sucrose and centrifuged for 5 min at 2500 rpm using a Sorvall HB-4 rotor. The supernatant was transferred to a clean tube and the flagella were collected by centrifugation for 10 min in the HB-4 rotor at 9224 ***g***. The pellet containing flagella was resuspended in 200 µl of HMDEK. Half of this final suspension was retained for use in light, immunofluorescence or electron microscopy, while 1 mM DTT (1,4-dithiothreitol), 2 mM Pefabloc SC (Sigma-Aldrich), and 25 µl 5X loading buffer (312.5 mM TRIS, pH 6.8, 10% sodium dodecyl sulfate, 25% β-mercaptoethanol, 50% glycine, and a small amount of Pyronin-Y) were added to the remaining 100 µl of flagella. The samples were then boiled for 5 min prior to being stored at −20°C for later SDS-PAGE and immunoblotting procedures.

Genomic analysis

The *C. reinhardtii* FMG-1B sequence, accession number Cre09.g392867, was obtained from Phytozome v12.1.6 (https://phytozome.jgi.doe.gov/pz/portal.html#). The *Chlamydomonas* Library Project provided details on the location of the insertion sequence within the 5′-UTR region of strain 56 and the 3′-UTR region of strain 47 (https://www.chlamylibrary.org/). Primers flanking the predicted insertion sites were designed using SnapGene (http://www.snapgene.com/) and synthesized by Integrated DNA Technologies (Skokie, IL). Genomic DNA was isolated from wt, 47, and 56 strains using phenol:chloroform (Newman et al., 1990). Modifications to the protocol were as described at the *Chlamydomonas* Resource Center (https://www.chlamycollection.org/methods/minipreps-of-dna-from-chlamydomonas-cultures/). For maximum extraction efficiency, several milliliters of cells were removed from flasks and centrifuged for 5 min at 2500 rpm with a Sorvall HB-4 rotor. Sedimented cells were resuspended in 500 µl of M medium before beginning the extraction procedure. PCR analysis was used to verify the presence of DNA insertions in mutant strains 47 and 56. PCR was performed with 500 ng of genomic DNA. A Thermo Fisher Scientific (Waltham, MA) Nanodrop 2000 spectrophotometer was used to quantify DNA concentrations for PCR. PCR was conducted with the Epicentre (Madison, WI) Failsafe™ PCR system K premix and enzyme mix. Because the *Chlamydomonas* genome has a high GC content, the premix was supplemented with high GC buffer (New England Biolabs, Ipswich, MA). Primers for amplification of the 5′-UTR were forward, 5′-CTTAGATCA-CCGCTCCG-3′ and reverse, 5′-CTGCGATTGGGTTGCACAAA-3′. The primers for amplification of the 3′-UTR were forward, 5′-TGTTACCTA-CACAAGGGGGC-3′ and reverse, 5′-TAGGTTGCACGTGTGA-3′. Thermocycler conditions were followed according to the Epicentre protocols for FailSafe™ mixes. Elongation time was increased to 4 min in an attempt to accommodate the size of the insertion cassette. Agarose gel electrophoresis was used to visualize the PCR data. Samples were run on a 1% agarose gel in TAE (40 mM Tris-HCl pH 7.6, 20 mM acetic acid, 1 mM EDTA) at 100 V for 50 min and stained with ethidium bromide for 40 min. Gels were rinsed in distilled water for 10 min and viewed with a UVP Imaging System (Upland, CA) to generate digital images.

SDS-PAGE and immunoblotting

SDS-PAGE was performed (Laemmli, 1970) using an 8% separating gel and a 3% stacking gel. Proteins were transferred to nitrocellulose membrane and blocked in TBS (50 mM Tris-HCl pH 7.5, and 150 mM NaCl) containing 5% nonfat dry milk and 0.02% sodium azide for 1 h. A 1:35,000 dilution of FMG-1B antibody #61, available from the Developmental Studies Hybridoma Bank (http://dshb.biology.uiowa.edu/), was prepared in TBS blocking buffer and placed on the blot for 1 h at room temperature with

gentle agitation. The membrane was washed three times for 10 min each in TBST (TBS+0.05% Tween-20). The blot was then incubated in a 1:50,000 dilution of goat anti-mouse antibody conjugated to horseradish peroxidase (Thermo Fisher Scientific, cat. no. A16072) in TBS containing 5% nonfat dry milk for 30 min with gentle agitation. The membrane was washed three times for 10 min each in TBST. Bio-Rad Clarity™ Western ECL Substrate (Bio-Rad, Hercules, CA) was used to detect chemiluminescence according to the manufacturer's protocol. Antibodies were stripped from the membrane by the mild stripping buffer wash cycle described by Abcam (Cambridge, MA; http://www.abcam.com/protocols/western-blot-membrane-stripping-for-restaining-protocol). The stripped membrane was blocked as above and then exposed to a 1:15,000 dilution of a monoclonal anti-α-tubulin antibody (Sigma-Aldrich Corp., St. Louis, MO, catalogue no. T9026) in blocking buffer for 1 h with gentle agitation. The membrane was washed three times for 10 min each in TBST. A second incubation was performed with goat anti-mouse-IgG antibody conjugated to horseradish peroxidase, diluted 1:30,000 in TBS containing 5% nonfat dry milk, for 30 min with gentle agitation. The membrane was washed three times for 10 min each in TBST. Bio-Rad Clarity™ Western ECL Substrate (Bio-Rad, Hercules, CA) was used to detect chemiluminescence according to the manufacturer's protocol.

DIC, fluorescence, and electron microscopy

Light-microscope observations were made using differential interference contrast (DIC) and/or fluorescence microscopy with an Axioskop 2 mot plus microscope with a 63×/1.4 numerical aperture Plan Apochromatic objective (Carl Zeiss, Inc., Thornwood, NY). An Optivar lens was used at 1× or 2× magnification depending on the procedure being conducted. The microscope projected images to a Hamamatsu ORCA-ER camera (Bridgewater, NJ). MetaMorph Software (Molecular Dynamics, Sunnyvale, California) was used to control the microscope, illumination shutters, and camera. The immunofluorescence protocol outlined in Mizuno and Sloboda (2017) was used with the following alterations: isolated flagella were resuspended in 3.7% formaldehyde in PBS and applied in 30 µl aliquots to 10-well microscope slides previously coated with 1% polyethyleneimine. After 10 min, the wells were aspirated and 1% Triton X-100 in phosphate-buffered saline (137 mM NaCl, 2.7 mM KCl, 10 mM NaH_2PO_4, 1.8 mM K_2HPO_4, pH 7.4) was added for 10 min at room temperature. The wells were washed three times with PBS and incubated for 15 min in blocking buffer (PBS containing 5% nonfat dry milk and 0.02% sodium azide). The wells were then washed once with PBS and exposed to FMG-1B antibody #8, available from the Developmental Studies Hybridoma Bank (http://dshb.biology.uiowa.edu/), for 1 h at a 1:1000 dilution in PBS. Samples were washed three times with PBS and exposed to donkey anti-mouse-IgG antibodies labeled with Cy3 for 40 min at a 1:200 dilution in PBS. The samples were washed three times with PBS and mounted in Prolong Gold Antifade Reagent (Life Technologies, Eugene, OR) for viewing.

For transmission electron microscopy, sedimented flagellar samples were overlaid with 2% glutaraldehyde in HMDEK buffer at room temperature for 1 h and then overnight in 2% glutaraldehyde in 0.1 M sodium cacodylate buffer, pH 7.4, at room temperature. Samples were post-fixed in 2% OsO_4 in Na cacodylate, pH 7.4, rinsed in distilled water, and dehydrated through an ethanol series (30, 50, 70, 85 and 95%, 15 min each). After three 15 min incubations in 100% ethanol, followed by two in propylene oxide, samples were embedded in LX-112 and sectioned. Sections on copper grids were then stained with 2% uranyl acetate in 50% ethanol followed by 0.2% Reynold's lead citrate and viewed with a JEOL JEM-1010 electron microscope (JEOL USA, Peabody, MA).

Flagellar regeneration

A sample of cells with full-length flagella was fixed by the addition of an equal volume of 2% glutaraldehyde in HMDEK to serve as a length control. Live cells in M medium were then collected by centrifugation for 5 min at 1025 ***g*** using a Sorvall HB-4 rotor. The supernatant was discarded, and the pellet was resuspended in TAP medium. Full-length flagella were detached from the cell body by performing a pH shock as described above. The supernatant was discarded and the cell pellet was resuspended in 50 ml of M medium; when working with the insertional mutant strains 47 and 56, the M medium also contained 20 µg/ml paromomycin. Cells were aerated and illuminated to allow flagellar regeneration. At intervals of 15, 30, 60, 90, 180 and 300 min, a 40 µl sample was removed and fixed by the addition of 40 µl of 2% glutaraldehyde in HMDEK buffer. The length of the regenerating flagella was measured using the Region Measurement function in MetaMorph, after having calibrated the imaging system with a stage micrometer. Fifty flagella were measured at each time point for all strains.

Microsphere movement assay

A sample of cells with full-length flagella growing in M medium was centrifuged for 5 min in an HB-4 rotor at 2500 rpm. Cells were resuspended in the same volume of TAP medium. A Nexcelom Biosciences (Lawrence, MA) Cellometer™ Auto T4 bright-field cell counter was used to ensure that the cell concentrations of the three strains were similar when conducting the procedure to ensure a similar comparison. Polystyrene microspheres (Polysciences, Inc., Warrington, PA, cat. no. 07306) having a diameter of 0.356 µm were used to assay microsphere binding and movement (Bloodgood, 1977). The ratio of microspheres to cells was kept constant for each strain examined, and the ratio of microspheres to cells was chosen so there were multiple cells per field of view, and numerous microspheres per field. Slides and cover slips were cleaned as described for the gliding assay. Each slide was viewed for a maximum of 5 min in order to prevent dehydration from affecting the results. Flagella were categorized based on the number of attached microspheres and the number of attached microspheres in motion along the flagella at the time of observation.

Gliding motility assay

Slides and cover slips were cleaned by immersion in 1 M HCl at room temperature for 1 h. This was followed by a rinse in deionized (DI) water and immersion in 50% ethanol at room temperature for 1 h. Slides and coverslips were then washed with DI water a second time and dried overnight in a covered, dust-free container. Cells were mounted onto the slides and observed by DIC microscopy for no longer than 5 min. During this time, cells were counted as either being in the gliding configuration (the two flagella on a single cell oriented 180° to each other) or not in the gliding configuration (the two flagella at an orientation other than 180° to each other).

Acknowledgements

We thank Munaya Sa'eed for expert assistance in the laboratory and Keith Kozminski (University of Virginia) for providing useful suggestions on an early version of the manuscript. This study was made possible by the generation of the CLiP library (Li et al., 2016), from which the mutant strains in this study were obtained.

Competing interests

The authors declare no competing or financial interests.

Author contributions

Conceptualization: R.A.B., R.D.S.; Methodology: R.A.B., J.T., R.D.S.; Validation: R.D.S.; Formal analysis: R.A.B., R.D.S.; Investigation: J.T., R.D.S.; Resources: R.D.S.; Data curation: R.D.S.; Writing - original draft: R.A.B., R.D.S.; Writing - review & editing: R.A.B., J.T., R.D.S.; Supervision: R.D.S.; Project administration: R.D.S.; Funding acquisition: R.D.S.

Funding

This work was made possible by a Dartmouth FRPDF (faculty research and professional development fund) generously provided by the Dean of the Faculty and by the Ira Allen Eastman (Class of 1829) Professorship, which was established in 1910 by a gift to the College from his widow, Jane Eastman.

Supplementary information

Supplementary information available online at
http://jcs.biologists.org/lookup/doi/10.1242/jcs.233429.supplemental

References

Bardele, C. F. (1976). Particle movement in heliozoan axopods associated with lateral displacement of highly ordered membrane domains. *Z. Naturforsch.* **321C**, 190-194. doi:10.1515/znc-1976-3-418

Belzile O., Hernandez-Lara C. I., Wang Q. and Snell W. J. (2013). Regulated membrane protein entry into flagella is facilitated by cytoplasmic microtubules and does not require IFT. *Curr Biol.* **23**, 1460-1465. doi:10.1016/j.cub.2013.06.025

Bessen, M., Fay, R. B. and Witman, G. B. (1980). Calcium control of waveform in isolated flagellar axonemes of Chlamydomonas. *J. Cell Biol.* **86**, 446-455. doi:10.1083/jcb.86.2.446
Betleja, E. (2012). Analysis of the gliding machinery in the green alga, Chlamydomonas reinhardtii. *Ph. D. dissertation*, University of Idaho. ProQuest #3536681.
Bloodgood, R. A. (1977). Motility occurring in association with the surface of the Chlamydomonas flagellum. *J. Cell Biol.* **75**, 983-989. doi:10.1083/jcb.75.3.983
Bloodgood, R. A. (1980). Direct visualization of dynamic membrane events in cilia. *J. Exptl. Zool.* **213**, 293-295. doi:10.1002/jez.1402130218
Bloodgood, R. A. (1981). Flagella-dependent gliding motility in Chlamydomonas. *Protoplasma* **106**, 183-192. doi:10.1007/BF01275550
Bloodgood, R. A. (1990). Gliding motility and flagellar glycoprotein dynamics in chlamydomonas. In *Ciliary and Flagellar Membranes* (ed. R. A. Bloodgood), pp. 91-128. Boston, MA: Springer US.
Bloodgood, R. A. (1992). Calcium-regulated phosphorylation of proteins in the membrane-matrix compartment of the Chlamydomonas flagellum. *Exptl. Cell Res.* **198**, 228-236. doi:10.1016/0014-4827(92)90375-I
Bloodgood, R. A. (2009). The Chlamydomonas flagellar membrane and its dynamic properties. In *The Chlamydomonas Source Book* (ed. George Witman), vol. 3, 2nd edn. pp. 309-368. Academic Press, N.Y.
Bloodgood, R. A. and May, G. S. (1982). Functional modification of the Chlamydomonas flagellar surface. *J. Cell Biol.* **93**, 88-96. doi:10.1083/jcb.93.1.88
Bloodgood, R. A. and Salomonsky, N. L. (1989). Use of a novel Chlamydomonas mutant to demonstrate that flagellar glycoprotein movements are necessary for the expression of gliding motility. *Cell Motil. Cytoskel.* **13**, 1-8. doi:10.1002/cm.970130102
Bloodgood, R. A. and Salomonsky, N. L. (1990). Calcium influx regulates antibody-induced glycoprotein movements within the Chlamydomonas flagellar membrane. *J. Cell Sci.* **96**, 27-33.
Bloodgood, R. A. and Salomonsky, N. L. (1991). Regulation of flagellar glycoprotein movements by protein phosphorylation. *Eur. J. Cell Biol.* **54**, 85-89.
Bloodgood, R. A. and Salomonsky, N. L. (1994). The transmembrane signaling pathway involved in directed movements of Chlamydomonas flagellar membrane glycoproteins involves the dephosphorylation of a 60-kD phosphoprotein that binds to the major flagellar membrane glycoprotein. *J. Cell Biol.* **127**, 803-811. doi:10.1083/jcb.127.3.803
Bloodgood, R. A. and Salomonsky, N. L. (1998). Microsphere attachment induces glycoprotein redistribution and transmembrane signaling in the Chlamydomonas flagellum. *Protoplasma* **202**, 76-83. doi:10.1007/BF01280876
Bloodgood, R. A. and Workman, L. J. (1984). A flagellar surface glycoprotein mediating cell-substrate interaction in Chlamydomonas. *Cell Motil.* **4**, 77-87. doi:10.1002/cm.970040202
Bloodgood, R. A., Leffler, E. M. and Bojczuk, A. T. (1979). Reversible inhibition of Chlamydomonas flagellar surface motility. *J. Cell Biol.* **82**, 664-674. doi:10.1083/jcb.82.3.664
Bloodgood, R. A., Woodward, M. P. and Salomonsky, N. L. (1986). Redistribution and shedding of flagellar membrane glycoproteins visualized using an anti-carbohydrate monoclonal antibody and concanavalin A. *J. Cell Biol.* **102**, 1797-1812. doi:10.1083/jcb.102.5.1797
Bowser, S. S. and Bloodgood, R. A. (1984). Evidence against surf-riding as a general mechanism for surface motility. *Cell Motil.* **4**, 305-314. doi:10.1002/cm.970040502
Bowser, S., Israel, H., Mcgeerussell, S. and Rieder, C. (1984). Surface transport properties of heticulopodia: Do intracellular and extracellular motility share a common mechanism? *Cell Biol. Internl. Rep.* **8**, 1051-1063. doi:10.1016/0309-1651(84)90092-4
Gebauer, F., Preiss, T. and Hentze, M. W. (2012). From Cis-regulatory elements to complex RNPs and back. *Cold Spring Harb. Perspect. Biol.* **4**, 1-14. doi:10.1101/cshperspect.a012245
Glöckner, G., Hülsmann, N., Schleicher, M., Noegel, A. A., Eichinger, L., Gallinger, C., Pawlowski, J., Sierra, R., Euteneuer, U., Pillet, L. et al. (2014). The Genome of the Foraminiferan Reticulomyxa filosa. *Curr. Biol.* **24**, 11-18. doi:10.1016/j.cub.2013.11.027
Hoffman, J. L. and Goodenough, U. W. (1980). Experimental dissection of flagellar surface motility in Chlamydomonas. *J. Cell Biol.* **86**, 656-665. doi:10.1083/jcb.86.2.656
Huang, K., Diener, D. R., Mitchell, A., Pazour, G. J., Witman, G. B. and Rosenbaum, J. L. (2007). Function and dynamics of PKD2 in Chlamydomonas reinhardtii flagella. *J. Cell Bio.* **179**, 501-514. doi:10.1083/jcb.200704069
Huttenlocher, A. and Horwitz, A. R. (2011). Integrins in cell migration. *Cold Spring Harb. Perspect. Biol.* **3**, 1-16. doi:10.1101/cshperspect.a005074
Hirano, T., Katoh, Y. and Nakayama, K. (2017) Intraflagellar transport-A complex mediates ciliary entry and retrograde trafficking of ciliary G protein-coupled receptors. *Mol. Biol. Cell* **28**, 429-439. doi:10.1091/mbc.E16-11-0813
Kamiya, R., Shiba, K., Inaba, K. and Kato-Minoura, T. (2018). Release of sticky glycoproteins from chlamydomonas flagella during microsphere translocation on the surface membrane. *Zool. Sci.* **35**, 299-305. doi:10.2108/zs180025
Kanno, F. and Ishii, K. (1979). Movement of the surface layer on axopodium and its protoplasm in Actinosphaerium. *Bull. Faculty of Liberal Arts Hosei Univ.* **31**, 1-8.
Kawachi, M., Inouye, I., Maeda, O. and Chihara, M. (1991). The haptonema as a food-capturing device: observations on Chrysochromulina hirta (Prymnesiophyceae). *Phycologia* **30**, 563-573. doi:10.2216/i0031-8884-30-6-563.1
Kozminski, K. G. (1995). Beat-independent flagellar motilities in Chlamydomonas and an analysis of the function of alpha-tubulin acetylation. *Ph. D. dissertation*, Yale University. ProQuest #9541435.
Kozminski, K. G., Johnson, K. A., Forscher, P. and Rosenbaum, J. L. (1993). A motility in the eukaryotic flagellum unrelated to flagellar beating. *Proc. Natl. Acad. Sci. USA* **90**, 5519-5523. doi:10.1073/pnas.90.12.5519
Kozminski, K. G., Beech, P. L. and Rosenbaum, J. L. (1995). The Chlamydomonas kinesin-like protein FLA10 is involved in motility associated with the flagellar membrane. *J. Cell Biol.* **131**, 1517-1527. doi:10.1083/jcb.131.6.1517
Laemmli, U. K. (1970). Cleavage of structural proteins during the assembly of the head of bacteriophage T4. *Nature* **227**, 680-685. doi:10.1038/227680a0
Laib, J. A., Marin, J. A., Bloodgood, R. A. and Guilford, W. H. (2009). The reciprocal coordination and mechanics of molecular motors in living cells. *Proc. Natl. Acad. Sci. USA* **106**, 3190-3195. doi:10.1073/pnas.0809849106
Lewin, R. A. (1952). Studies on the flagella of algae. I. General observations of Chlamydomonas moewusii Gerloff. *Biol. Bull.* **103**, 74-79. doi:10.2307/1538407
Lewin, R. A. (1982). A new kind of motility mutant (non-gliding) in Chlamydomonas. *Experientia* **38**, 348-349. doi:10.1007/BF01949384
Li, X., Zhang, R., Patena, W., Gang, S. S., Blum, S. R., Ivanova, N., Yue, R., Robertson, J. M., Lefebvre, P. A., Fitz-Gibbon, S. T. et al. (2016). An indexed, mapped mutant library enables reverse genetics studies of biological processes in Chlamydomonas reinhardtii. *Plant Cell* **28**, 367-387. doi:10.1105/tpc.15.00465
Mast, S. O. (1912). The reactions of the flagellate Peranema. *J. Anim. Behav.* **2**, 91-97. doi:10.1037/h0072097
Mizuno, K. and Sloboda, R. D. (2017). Protein arginine methyltransferases interact with intraflagellar transport particles and change location during flagellar growth and resorption. *Mol. Biol. Cell* **28**, 1208-1222. doi:10.1091/mbc.e16-11-0774
Morthorst, S. K., Christensen, S. T. and Pedersen, L. B. (2018) Regulation of ciliary membrane protein trafficking and signaling by kinesin motor proteins. *FEBS Journal*. **285**, 4535-4564.
Newman, S. M., Boynton, J. E., Gillham, N. W., Randolph-Anderson, B. L., Johnson, A. M. and Harris, E. H. (1990). Transformation of chloroplast ribosomal RNA genes in Chlamydomonas: molecular and genetic characterization of integration events. *Genetics* **126**, 875-888. doi:10.1111/febs.14583
Noda, N. and Tamm, S. L. (2014). Lithocytes are transported along the ciliary surface to build the statolith of ctenophores. *Curr. Biol.* **24**, R951-R952. doi:10.1016/j.cub.2014.08.045
Picariello, T., Brown, J. M., Hou, Y., Swank, G., Cochran, D. A., King, O. D., Lechtreck, K., Pazour, G. J. and Witman, G. B. (2019). A global analysis of IFT-A function reveals specialization for transport of membrane-associated proteins into cilia. *J. Cell Sci.* **132**, jcs220749. doi:10.1242/jcs.220749
Qin, H., Burnette, D. T., Bae, Y. K., Forscher, P., Barr, M. M. and Rosenbaum, J. L. (2005). Intraflagellar transport is required for the vectorial movement of TRPV channels in the ciliary membrane. *Curr. Biol.* **15**, 1695-1699. doi:10.1016/j.cub.2005.08.047
Reinhart, F. D. and Bloodgood, R. A. (1988). Membrane-cytoskeleton interactions in the flagellum: a 240,000 Mr surface-exposed glycoprotein is tightly associated with the axoneme in Chlamydomonas moewusii. *J. Cell Sci.* **89**, 521-531.
Rosenbaum, J. L. and Witman, G. B. (2002). Intraflagellar transport. *Nat. Rev. Molec. Cell Biol.* **3**, 813-825. doi:10.1038/nrm952
Sager, R. and Granick, S. (1953). Nutritional studies with Chlamydomonas reinhardi. *Ann. NY Acad. Sci.* **56**, 831-838. doi:10.1111/j.1749-6632.1953.tb30261.x
Saito, A., Suetomo, Y., Arikawa, M., Omura, G., Khan, S. M. M. K., Kakuta, S., Suzaki, E., Kataoka, K. and Suzaki, T. (2003). Gliding movement in Peranema trichophorum is powered by flagellar surface motility. *Cell Motil.* **55**, 244-253. doi:10.1002/cm.10127
Schmidt, J. A. and Eckert, R. (1976). Calcium couples flagellar reversal to photostimulation in Chlamydomonas reinhardtii. *Nature* **262**, 713-715. doi:10.1038/262713a0
Shih, S. M., Engel, B. D., Kocabas, F., Bilyard, T., Gennerich, A., Marshall, W. F. and Yildiz, A. (2013). Intraflagellar transport drives flagellar surface motility. *eLife Sci.* **2**, e00744. doi:10.7554/eLife.00744
Snell, W. J., Buchanan, M. and Clausell, A. (1982). Lidocaine reversibly inhibits fertilization in Chlamydomonas: a possible role for calcium in sexual signalling. *J .Cell Biol.* **94**, 607-612. doi:10.1083/jcb.94.3.607
Stepanek, L. and Pigino, G. (2016). Microtubule doublets are double-track railways for intraflagellar transport trains. *Science* **352**, 721-724. doi:10.1126/science.aaf4594
Suzaki, T., Shigenaka, Y., Watanabe, S. and Toyohara, A. (1980). Food capture and ingestion in the large heliozoan, Echinosphaerium nucleofilum. *J. Cell Sci.* **42**, 61-79.
Troyer, D. (1975). Possible involvement of the plasma membrane in saltatory particle movement in heliozoan axopods. *Nature* **254**, 696-698. doi:10.1038/254696a0
Ulehla, V. V. (1911). Ultramikroskopische Studien uber Geisselbewegung. *Biol. Zent. Bl.* **31**, 689-705.

Witman, G. B., Carlson, K., Berliner, J. and Rosenbaum, J. L. (1972). Chlamydomonas flagella. I. Isolation and electrophoretic analysis of microtubules, matrix, membranes, and mastigonemes. *J. Cell Biol.* **54**, 507-539. doi:10.1083/jcb.54.3.507

Ye, F., Breslow, D. K., Koslover, E. F., Spakowitz, A. J., Nelson, W. J. and Nachury, M. V. (2013). Single molecule imaging reveals a major role for diffusion in the exploration of ciliary space by signaling receptors. *eLife*. **2**, e00654. doi:10.7554/elife.00654

Supplementary Material

Figure S1

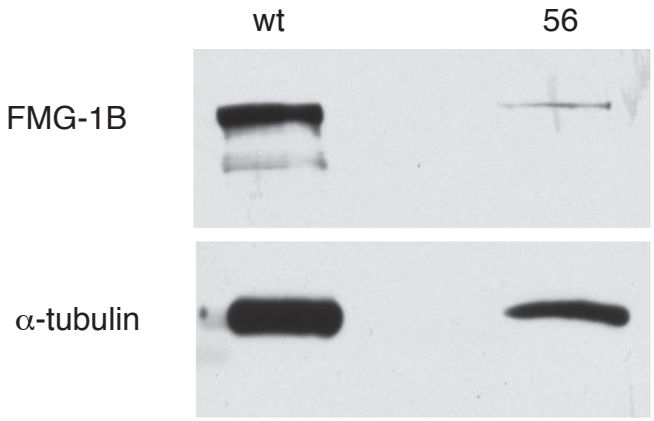

Figure S1. Variability in FMG-1B Expression in the Strain 56 Insertional Mutant

This figure demonstrates that, on occasion, a small quantity of FMG-1B protein can be detected via immunoblotting with FMG-1B antibodies (#61) in samples of flagella isolated from strain 56 cells. The blot was stripped and then reprobed with α-tubuilin antibodies to serve as a loading control.

Figure S2

wt

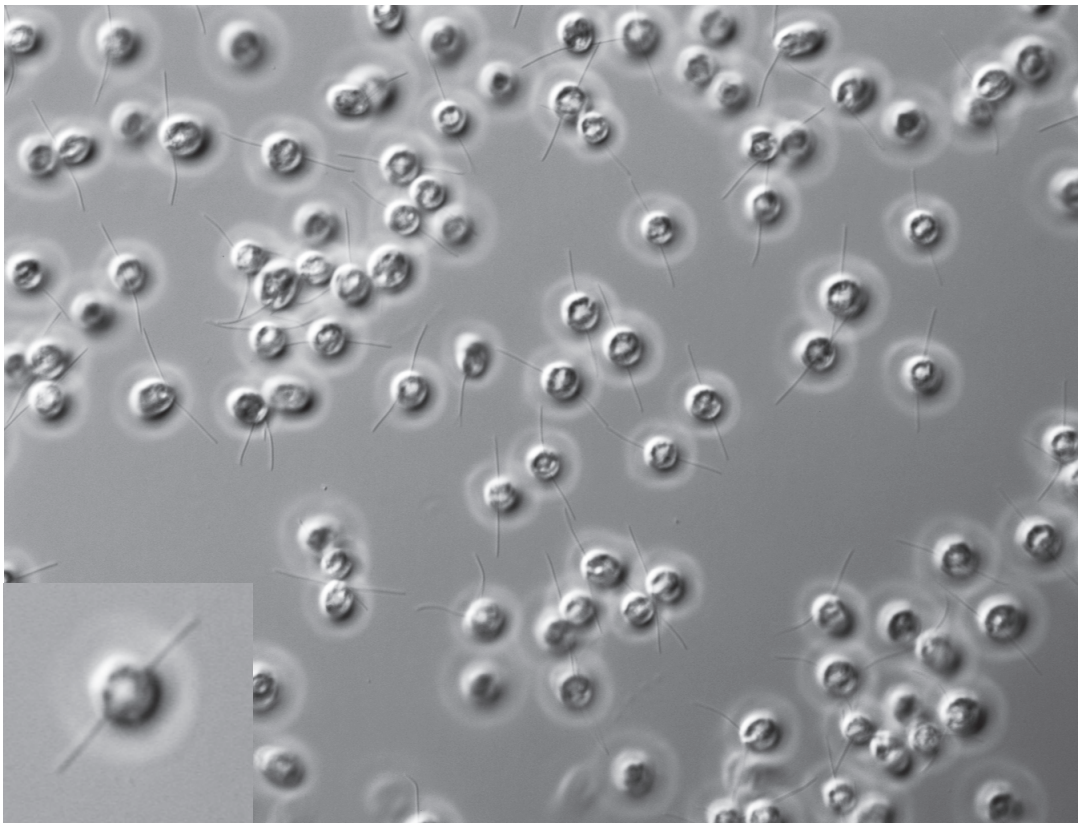

56

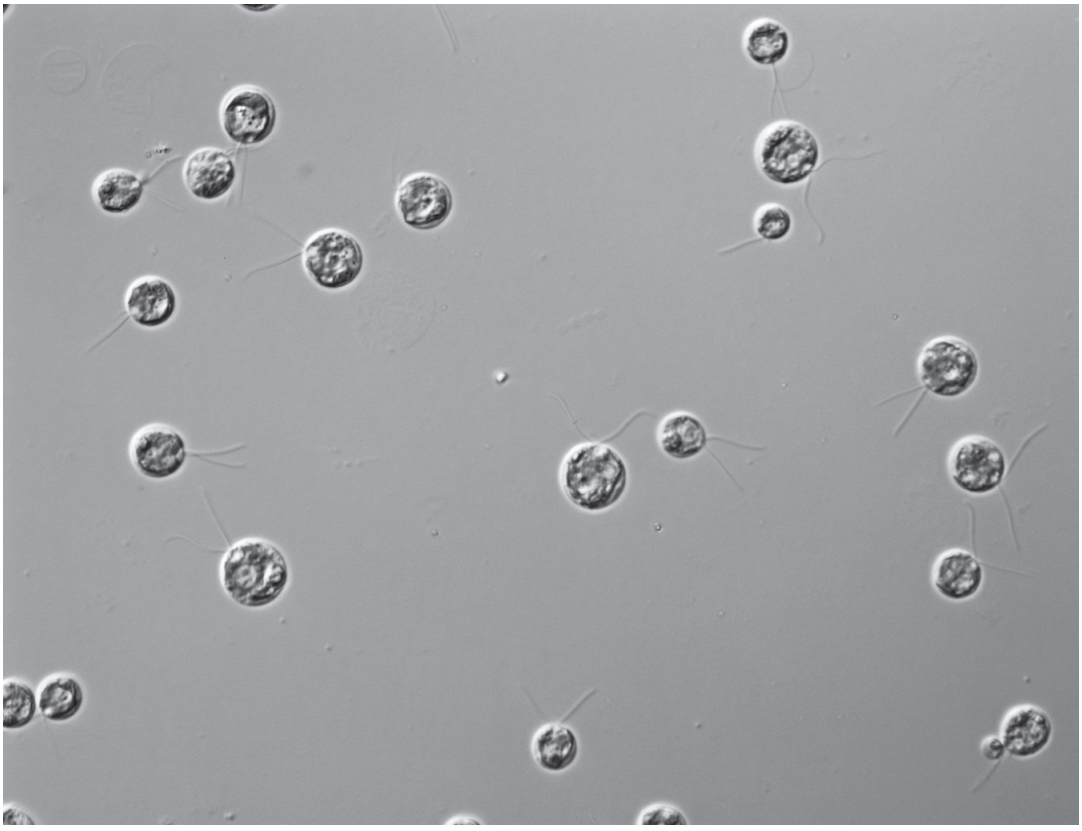

Figure S2. Representative microscope fields showing DIC images of wt and strain 56 cells with their flagella in various positions relative to the cell body. The inset in the upper panel shows an enlarged image of one wt cell that has adopted the gliding morphology (flagella positioned 180° to each other). The brightness and contrast of these images has been uniformly enhanced by setting these controls in Adobe Photoshop to a value of 80 for each. This manipulation was performed to render the images of the flagella more readily apparent.

Movie 1. This movie demonstrates the movement of polystyrene microspheres along the flagellum. Images were acquired at a rate of one image per 111 msec, or nine images (*i. e.* frames) per second. The video displays at 30 frames per second, and thus the movie shows microsphere movement at 3.3x greater than normal speed.